International Journal of Coal Science & Technology (2022) 9:80
https://doi.org/10.1007/s40789-022-00549-2

RESEARCH

Determination of mining-induced stresses using diametral rock core deformations

Yizhuo Li[1] · **Hani S. Mitri**[1]

Received: 21 February 2022 / Accepted: 1 September 2022

Abstract
Knowledge of ground stresses is crucial for ground control activities such as the design of underground openings, selection of support systems, and analysis for stability. However, it is a known fact that far field stresses experience changes in orientation and magnitude due to the presence of geological structures and due to the excavations created by mining activities. As a result, in-situ stresses around drifts, ramps, and stopes in underground mines are quite different from far field or pre-mining stresses. The purpose of this research is to develop a simple and practical methodology for determining in-situ stresses. Stress relief occurs once the rock core is drilled off. Such relief is a function of the surrounding stress field. This study uses exploration rock cores that are drilled off for the purpose of orebody definition in the underground mine. The method measures and analyzes the diametral core deformations in laboratory. Two case studies from operating underground mines are presented for demonstration. In these case studies, rock core deformations are measured with a customized test apparatus and rock samples were prepared and tested for Young's modulus and Poisson's ratio. The differential stress, namely the difference between the local principal stresses in the plane perpendicular to the core rock axis is calculated. It is shown that this methodology is useful for determining the brittle shear ratio in the rock mass, which is of primary interest to ground control studies.

Keywords In-situ stresses · Rock core diametral deformation · Strain relief · Core-based stress measurement · Brittle shear ratio

1 Introduction

There are numerous, well-established in-situ stress measurement techniques that are being used in practice. The knowledge of in-situ stresses is important for both engineering analysis and design. In underground excavations, the in-situ stress regime can greatly affect stability, and it is also one of the most important boundary conditions for the analysis. Existing widely used in-situ stress methods include over-coring and hydraulic fracturing (Amadei 1984). However, such methods can be expensive, laborious, and time-consuming.

In underground mining applications, in-situ stresses change with the underground activities such as drift development and stope extraction. Stress changes are not only influenced by the size and shape of underground excavations. They are also influenced by the presence of geological features such as faults, shear zones, foliations, and others. This makes it extremely difficult to predict and verify the changes of in-situ stresses even with the use of advanced numerical models (Kaiser et al. 2000). Hence, investigating the development of an effective and practical method to estimate excavation-induced stresses should prove useful in practice. The approach presented in this study and applied to underground mining, can be adapted to other engineering applications such as civil engineering shafts and tunnels in hydro power and transit projects.

There are three major categories of in-situ stress measurement. They are destructive, semi-destructive, and non-destructive methods. Hydraulic fracturing is one example of destructive methods, whereas over-coring is an example of semi-destructive methods. The diametral rock core analysis includes extracting and analyzing rock core deformations due to stress/strain relief in laboratory is considered a non-destructive approach. Strain relief occurs once the rock core is drilled off; the relief is a function of the surrounding stress

✉ Yizhuo Li
yizhuo.li@mail.mcgill.ca

1 Department of Mining and Materials Engineering, McGill University, Montreal, Canada

Published online: 24 October 2022

field (Brady and Brown 2006). Although all approaches require high level of precision, it is relatively easier to take precision measurements in the laboratory rather than in the harsh environment of the mine site. This study adopts the non-destructive approach; it uses exploration rock cores that are drilled off primarily for the purpose of orebody definition. An experimental setup has been built to measure and analyze the diametral core deformations in laboratory. This study aims to show how rock core diametrical deformation analysis can be employed to determine the differential stress or the brittle shear ratio in the rock mass.

In the case studies presented herein, the rock samples are retrieved from depths of 1.3 to 1.8 km below surface. The influence of core size on the accuracy of the results when applying diametrical core deformation analysis is discussed Also, the relation between differential stresses and depth is investigated.

2 Diametral rock core deformation

Figure 1 illustrates the process of strain relief in a rock core upon extraction. In Fig. 1a, the core diameter is before extraction d_0 and is subjected to local principal stresses σ_h, σ_H acting on a plane perpendicular to the core axis. Upon the extraction of the core, it expands due to stress relief to d_{max} and d_{min} as shown in Fig. 1b. Thus, by accurately surveying the profile of the rock core, it is possible to determine the magnitudes of the maximum and minimum diameters d_{max} and d_{min} as well as their orientation. Funato and Ito (2017) developed an analytical model based on the theory of linear elasticity for isotropic, homogenous, and continuous rock, which relates the maximum and minimum core diameters to the local principal stress field σ_h, σ_H. It is given by

$$\sigma_H - \sigma_h = \frac{E}{1+\nu}\frac{d_{max} - d_{min}}{d_o} \approx \frac{E}{1+\nu}\frac{d_{max} - d_{min}}{d_{min}} \tag{1}$$

where E and ν are Young's modulus and Poisson's ratio, respectively. Since only one equation is derived for the core deformation analysis, even with known rock properties only the differential stress and principal orientation can be determined.

This study is concerned with the application of Eq. (1) to underground mining. It focuses on estimating the local principal stress differential, $\sigma_H - \sigma_h$ (Fig. 2) located on a plane perpendicular to the core axis. In the special case when the core axis is oriented parallel to one of the principal in-situ stresses, the stresses σ_H and σ_h will automatically be the remaining in-situ principal stresses as shown in Fig. 2.

3 Experimental setup

This experiment aims to measure the deformation of rock core sample caused by stress relief and test the elastic rock properties. The experiment can be divided into two parts, namely, rock core diameter measurement and uniaxial compressive strength (UCS) test. The method of diameter measurement is by a laser micrometer and the objective is to determine the maximum and minimum diameters of the rock core samples and provide d_{max} and d_{min} by taking multiple measurements around the circumference of the rock core. The customized test apparatus has been designed to continuously measure the rock cores over 360° rotation with diameters from 30.5 mm (AQTK) to 85 mm (PQ), which covers the range of most used drill bit sizes in mining and exploration projects (Fig. 3). The UCS tests were performed as a second part of the experiment. After determining the maximum and minimum diameters, the rock samples were prepared for the UCS test for the mechanical properties Young's modulus and Poisson's ratio.

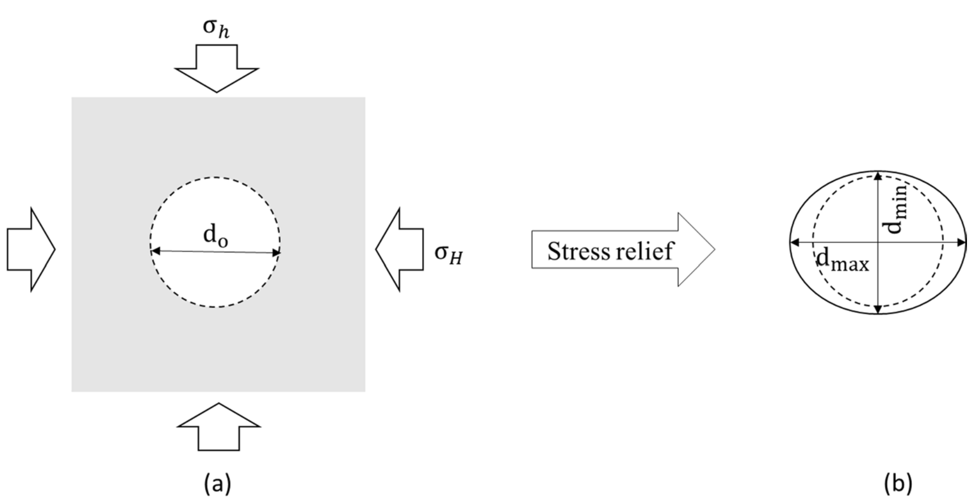

Fig. 1 Schematic of rock core relief: **a** Rockmass under biaxial stresses; **b** Rock core deformation after taking out

3.1 Sensitivity analysis

This study requires the measuring instrument to have high resolution to detect small diameter differences more accurately. Sensitivity analysis is performed to investigate how the output factors can be affected by the variation of input factors, and to help determine the required resolution of the micrometer used for measuring the sample diameters.

The base case results for the sensitivity analysis are calculated from the rock core dimensions of d_{max}= 47.61393 mm, d_{min} = 47.59205 mm, and d_0= 47.59155 mm, the elastic properties of Young's modulus and Poisson's ratio are 76.4 GPa and 0.174, respectively. The stress results of the base case are σ_H = 37.19 MPa and σ_h= 7.27 MPa. The sensitivity analysis results are compared with these base results. The aim of performing sensitivity analysis on the inputs d_{max} and d_{min} is to ensure that the outputs, stress results, are within an acceptable range of accuracy. Two sensitivity analyses are performed for two resolutions namely 0.00025 mm and 0.0001 mm in input diameters. Clearly, the higher resolution of input measurements would yield higher precision of stress calculation.

Table 1 shows the results of the sensitivity analysis for the resolution of 0.00025 mm, with case 1 being the base case. To assess the influence of errors due to measuring instrument resolution, four analyses are conducted and compared to the base case (Case 1 in Table 1). For each case, the principal stresses are calculated and compared with the base case stresses. The accuracy of the results is shown in $\%\sigma_H$ and $\%\sigma_h$. As can be seen from the results, the stress

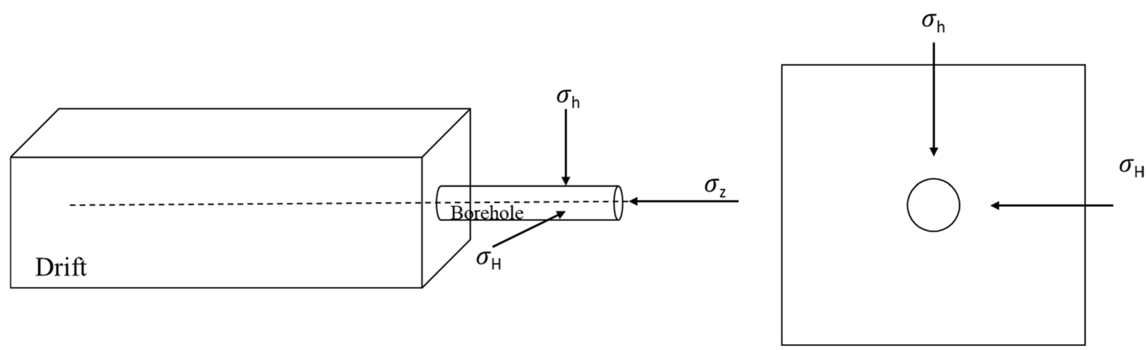

Fig. 2 Illustration of local stresses σ_H and σ_h to the extracted core axis

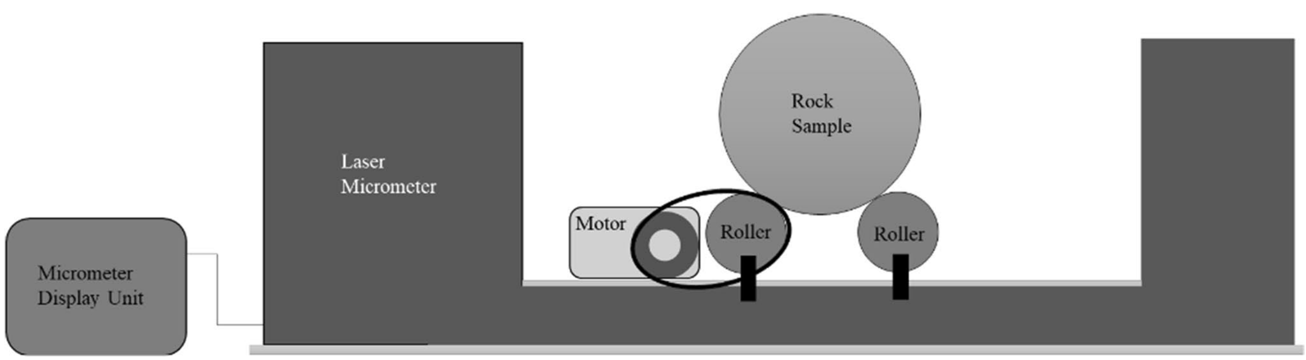

Fig. 3 Schematic of experiment for measuring the rock sample diameter

Table 1 ±0.00025 mm resolution results

Case	Tolerance in d_{max} (mm)	Tolerance in d_{max} (mm)	$\Delta\sigma_H$ (MPa)	$\Delta\sigma_h$ (MPa)	$\%\sigma_H$	$\%\sigma_h$
1	0.00000	0.00000	0.000	0.000	0.00	0.00
2	+0.00025	+0.00025	0.486	0.486	1.31	6.68
3	+0.00025	−0.00025	0.356	−0.263	0.96	−3.62
4	−0.00025	−0.00025	−0.472	−0.407	−1.27	−5.60
5	−0.00025	+0.00025	−0.342	0.342	−0.92	4.70

Table 2 ±0.0001 mm in diameters from nominal maximum and minimum diameters

Case	Tolerance in d_{max} (mm)	Tolerance in d_{max} (mm)	$\Delta\sigma_H$ (MPa)	$\Delta\sigma_h$ (MPa)	$\%\sigma_H$	$\%\sigma_h$
1	0.0000	0.0000	0.000	0.000	0.00	0.00
2	+0.0001	+0.0001	0.194	0.194	0.52	2.67
3	+0.0001	−0.0001	0.137	−0.137	0.37	−1.88
4	−0.0001	−0.0001	−0.102	−0.102	−0.27	−1.40
5	−0.0001	+0.0001	−0.137	0.137	−0.37	1.88

estimation error varies between − 5.6% and + 6.68% for the minor principal stress and between − 1.27% and + 1.31% for the maximum principal stress.

Table 2 shows the results of sensitivity analysis for measurement resolution of 0.0001 mm, with case 1 being the base case. Like the previous analysis, four cases (No. 2 to No. 5) are compared to the base case (No. 1). As can be seen in Table 2, the stress estimation error varies between − 1.40% and + 2.67% for the minor principal stress and between − 0.27% and + 0.52% for the maximum principal stress.

The comparison of the results in Tables 1 and 2 indicate that a measurement resolution of 0.0001 mm in d_{max} and d_{min} will yield more accurate results than a resolution of 0.00025 mm. The comparison also reveals that the minor principal stress values are more sensitive to measurement resolution than major principal stresses. More importantly, the maximum error in the calculation of the differential stress is reduced from more than 5% in Table 1 to only less than 2.3% in Table 2. In light of these results, it can be concluded that that the resolution of the micrometer instrument should not be inferior to ± 0.0001 mm. This will ensure that the principal stress calculations will be within a margin of error of ±3%.

3.2 Measurement apparatus

Based on the sensitivity analysis, a measuring equipment with 0.0001 mm resolution is necessary for the application of diametrical core deformation analysis. Thus, a laser micrometer system (measuring and display units) from Mitutoyo Corporation was acquired (Fig. 4).

Based on the experimental objective, the laser micrometer must have a measuring range that covers rock core diameters commonly encountered in mining exploration drilling. The range of diameters vary from 30.5 mm (AQTK) to 85 mm (PQ). Good repeatability is also important to provide reliable results in this study. The instrument and parts required for the laboratory measurement are summarized in Table 3 and illustrated in Fig. 5.

Two pairs of high-precision rollers with the same diameter are used to support and rotate the rock sample. The rollers can be either manually rotated or connected to a servo motor using a belt running at 0.7 rpm. A gap between the two pairs is left for the measuring space to allow the laser beam to be interrupted only by the core sample, see Fig. 6.

Four pairs of brackets are fabricated for the rollers. Each pair has two aligned holes at the bottom to ensure that the roller axis is perfectly perpendicular to the laser beam and to avoid any shakiness from occurring. Two customized aluminum base plates were designed. The first plate is used as a base for the laser micrometer whereas the second plate serves as a base supporting the rollers as shown in Fig. 6. The second plate has 4 sets of threaded holes along the lines to fasten the roller brackets along any of the lines A, B, C and D shown in Fig. 7. In this way, the roller pairs can be

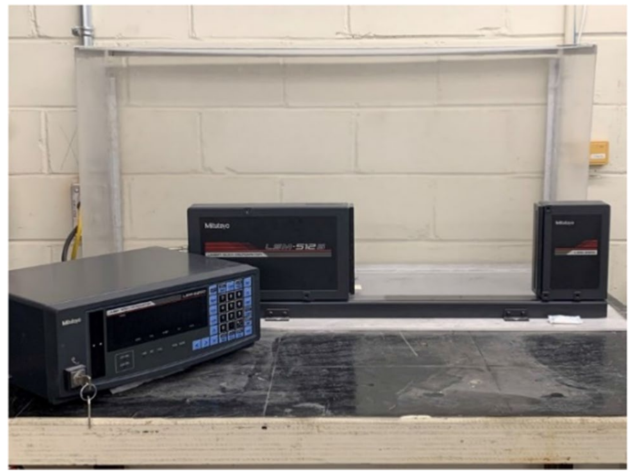

Fig. 4 Photo of LSM-512S laser micrometer with LSM 6200 display unit

Table 3 Summary of apparatus (refer to Fig. 5)

Item No.	Description	Quantity
1	Laser scan micrometer measuring unit	1
2	Micrometer display unit	1
3	Rollers	4
4	Bracket (roller support)	8
5	Base plate	2

Fig. 5 Apparatus of rock core diameter measurement with rock sample

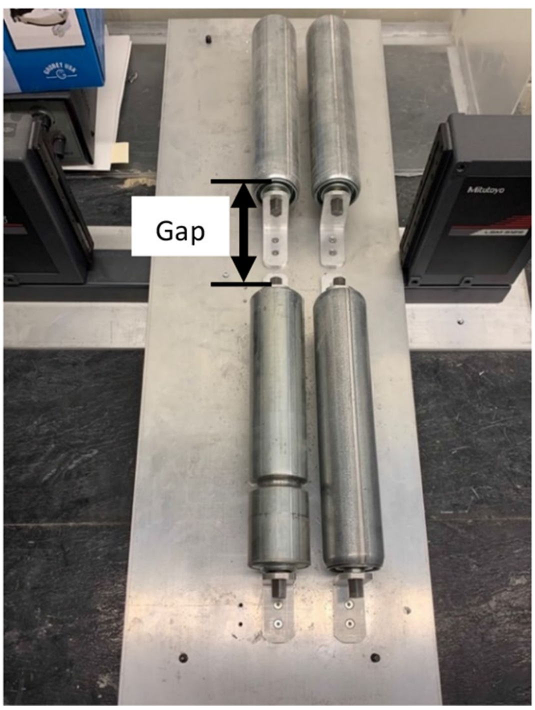

Fig. 6 Photograph showing the gap between the two pairs of rollers

positioned to accommodate different sizes of the rock cores, see Table 4.

3.3 Mechanical properties

The rock samples were prepared for the UCS test after the diameter measurement, and the test was conducted in accordance with ASTM D7012 to determine the rock mechanical properties namely uniaxial compressive strength, Young's

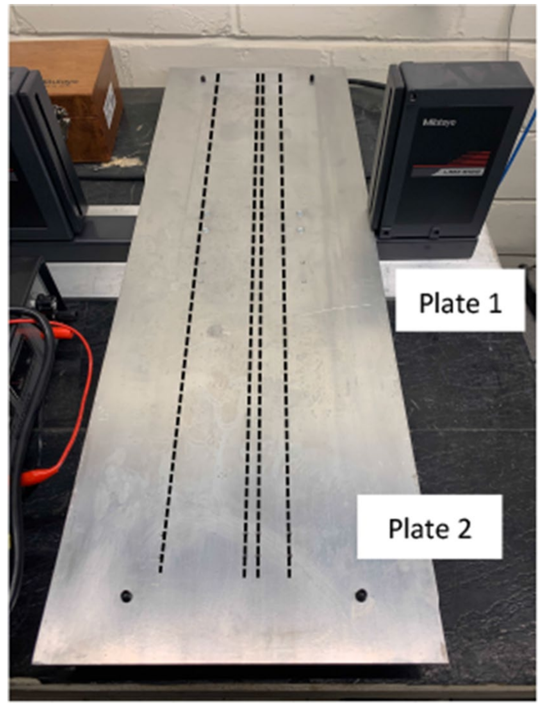

Fig. 7 Baseplates for the micrometer and rollers

Table 4 Roller position versus rock core size

Positions of roller pairs	Rock core size
A and B	AQTK, BQ
A and C	NQ, HQ
A and D	PQ

modulus, and Poisson's ratio. Testing was conducted using a hydraulic servo-controlled uniaxial press and data acquisition system. Two 120 Ohm strain gauges are installed on each specimen, one horizontal and one vertical for the elastic modulus test as shown in Fig. 8.

Based on ASTM D7012, the axial stress load must be applied between 0.5 and 1.0 MPa/s or the test duration before failure must be between 2 and 15 min. To do so, a pilot test with preferably a low loading rate of 0.2 MPa/s is needed to obtain a reasonable time estimate of the UCS. The test setup is shown in Fig. 9.

4 Stress analysis using rock core deformation

The application of diametrical core deformation analysis is presented with two case studies. The rock samples used in this study were collected from Fraser mine and Hoyle Pond mine. In Case study 1, rock core was extracted

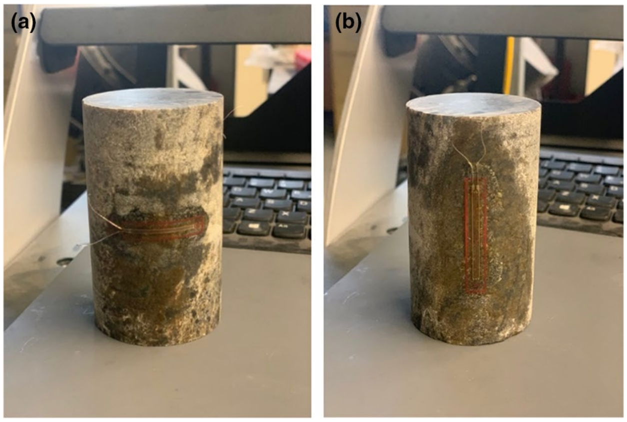

Fig. 8 Sample instrumentation: **a** Horizontal strain gauge; **b** Vertical strain gauge

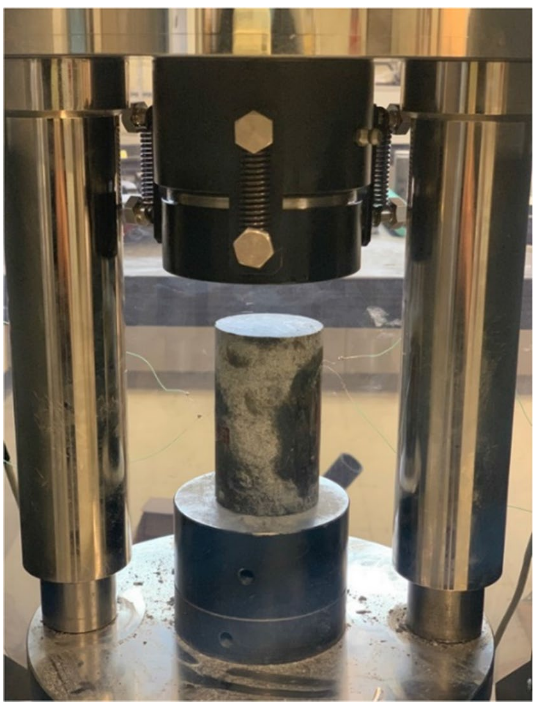

Fig. 9 Setup of UCS test

from Fraser mine. Rock core deformations were measured, and rock properties were tested to determine differential mining-induced stresses (Fig. 10). The results are then reported. In Case study 2, the same procedure as those used in Case study 1 is followed to implement the methodology for Hoyle Pond mine, and the relationship between differential stress and depth is investigated.

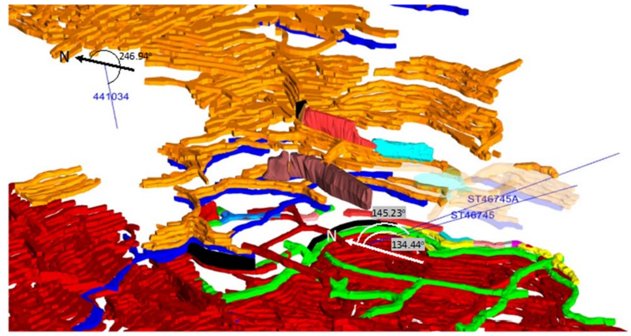

Fig. 10 3D view of a Fraser mine level 1340 m below surface

Table 5 Borehole orientations of case study 1

Borehole ID	Azimuth (°)	Dip (°)
ST46745	145.23	3.2
ST46745A	134.44	2.53
441034	246.94	− 38.15 (downward)

4.1 Case study 1—Fraser mine

The tested rock core samples from Fraser mine are obtained from three different boreholes located approximately 1340 m (4400 feet) below surface. Borehole orientations are listed in Table 5. Overburden stress can be estimated using Eq. (2). Considering a unit weight of rock of 0.028 MN/ m^3, the overburden pressure for this case is estimated to be 37.5 MPa.

$$\sigma_v = \gamma \cdot z. \tag{2}$$

4.1.1 Rock core deformation measurement

The samples of case study 1 were extracted from the three different boreholes by using two different sizes of drill bit: AQTK (30.5 mm) and NQ (47.6 mm). The sample deformations were measured using the laser micrometer system in Fig. 5, and the results are summarized in Table 6.

4.1.2 Orientation of principal stress

In general, if the gravity direction is marked (dashed line in Fig. 11) on the rock sample before drilling, the angle (θ) between gravity and the major principal stresses can be determined. The principal stress directions coincide with d_{max} and d_{min} (Fig. 11). The reliability of using rock core diametral deformation to determine the principal stress orientation has

Table 6 Measurement results of rock samples

Sample ID	Borehole ID	Rock Type	Drill Bit Size	d_{max} (mm)	d_{min} (mm)
ST46745-IGN-29	ST46745	Granite	AQTK	30.6112	30.5966
ST46745-FGN-7	ST46745	Felsic Gneiss	AQTK	30.5422	30.5277
ST46745-SDBX-52	ST46745	Sudbury Breccia	AQTK	30.5156	30.4948
ST46745A-DIA-51	ST46745A	Matachewan Diabase	AQTK	30.5767	30.5600
441034-SDBX-84	441034	Sudbury Breccia	NQ	47.6139	47.5921
441034-DIA-117	441034	Matachewan Diabase	NQ	47.4331	47.4150
441034-FGN-87	441034	Felsic Gneiss	NQ	47.6683	47.6321

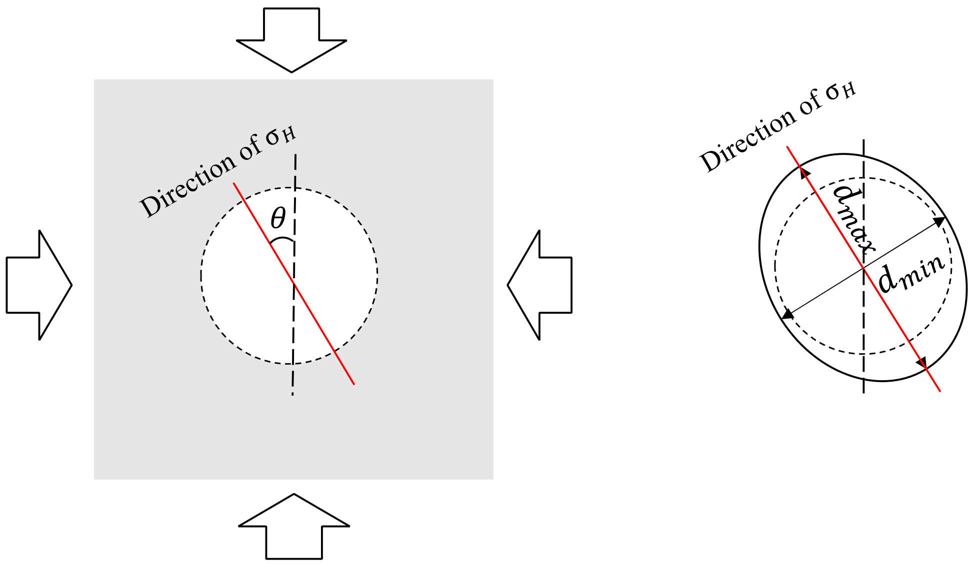

Fig. 11 Determination of principal stress orientation from rock core deformation

recently been investigated and confirmed by Ziegler and Valley (2021). However, the rock samples used in this study had no gravity direction mark. Thus, stress directions were only labeled on the samples rather than providing their orientation with respect to gravity mark. Some sample photos labeled with d_{max}(horizontal), the directions of σ_H and d_{min}(vertical), and the direction of σ_h are provided in Table 7.

As indicated in Table 7, d_{max} and d_{min} are nearly perpendicular to each other for the NQ samples. One of the AQTK samples (ID: ST46745A-DIA-51) is shown in Fig. 12. Each sample was measured three times (red lines). However, for the samples with a small diameter, such as AQTK (30.5 mm), the d_{max} and d_{min} labels from each measurement are scattered, and thus, determining the exact directions of σ_H and σ_h is difficult.

4.1.3 Results of Case study 1

The measured diameter values in Table 6 with rock properties that were obtained from UCS test can be directly applied to Eq. (1) to obtain the results of differential principal stress. For example, the NQ size Sudbury breccia rock core sample (ID: 441034-SDBX-84) was used to determine the differential stresses at Borehole 441034 from 84.5 m to 85 m. The principal stresses in the plane perpendicular to the borehole axis were investigated (see Plane A in Fig. 13). The measurement results are as follows: d_{max} = 47.6139 mm and d_{min} = 47.5921 mm. The elastic properties of the rock sample were obtained through UCS test, and the deformation measurement results are presented in Table 8. The differential stress for this sample is 31.3 MPa.

4.2 Case study 2—Hoyle Pond mine

The borehole information of rock samples provided by Hoyle Pond mine is presented in Table 9. A total of 19 samples were measured from two boreholes and extracted from 1357 and 1840 m below the surface by using NQ drill bit. The overburden pressure estimated from Eq. (2) for boreholes 25947 and 25986 is 36.6 MPa and 49.7 MPa, respectively.

Table 7 Front view of rock samples showing the orientation of principal diameters

Sample ID	NQ sample photo with labeled $d_{\max}$ (horizontal) and $d_{\min}$ (vertical)
441034-SDBX-84	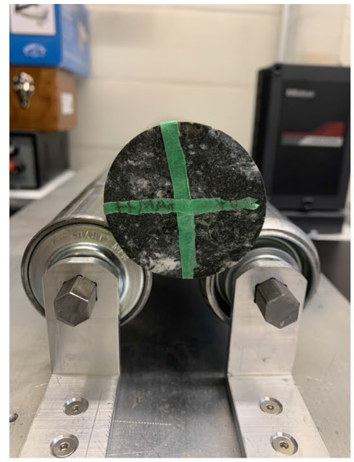
441034-DIA-117	
441034-FGN-87	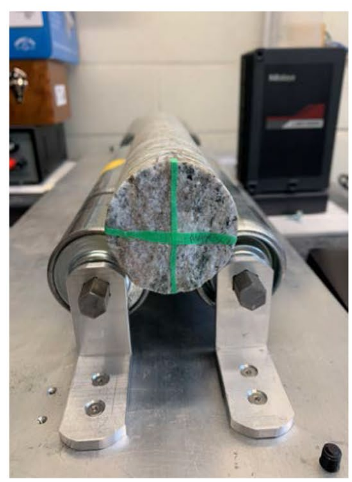

4.2.1 Rock core deformation measurement

The measurement results with rock types of Hoyle Pond mine rock cores are provided in Table 10.

The average difference between $d_{\max}$ and $d_{\min}$ in Table 10 is within the range of 0.013–0.058 mm, which is higher than that in the first case. This finding indicates that the difference in principal stresses in Case study 2 is larger than that

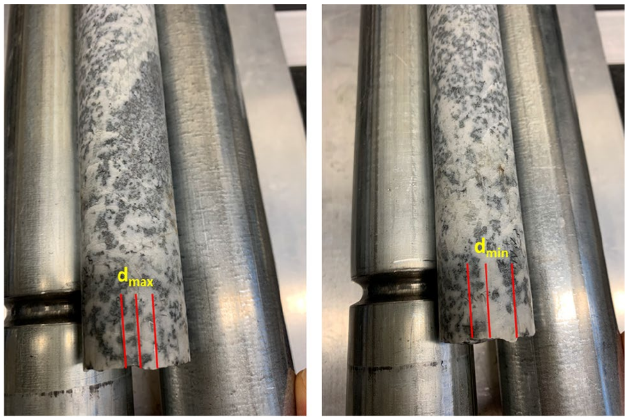

Fig. 12 Top view of ST46745A-DIA-51 showing location of measuring results

Table 8 Summary of laboratory test results (441034-SDBX-84)

Sample ID	d_{max} (mm)	d_{min} (mm)	E (GPa)	v
441034-SDBX-84	47.61393	47.59205	80.0	0.174

in Case study 1 (see results in Table 6). Also, it is noticed that the measured diameter results are significantly less than NQ core size (47.6 mm), which can be caused by different factors. One of them is due to material losses during the drilling process.

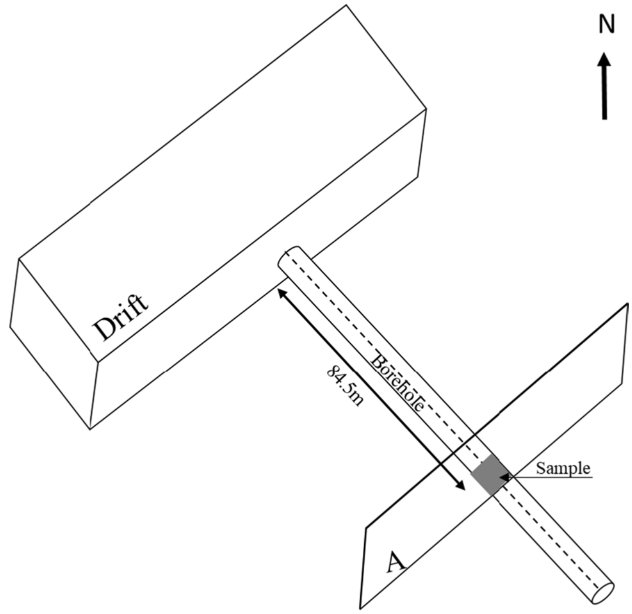

Fig. 13 Schematic showing the plane of stress calculations for hole 441034-SDBX-84

Table 9 Borehole orientations of case study 2

Borehole ID	Azimuth (°)	Dip (°)
25947	353	−3 (downward)
25986	33	−29 (downward)

Table 10 Measurement results of rock samples

Sample ID	Borehole ID	Rock type	Drill bit size	d_{max} (mm)	d_{min} (mm)
25947-0225-0	25947	High Fe Basalt	NQ	47.3908	47.3370
25947-0225-2	25947	High Fe Basalt	NQ	47.3410	47.3285
25947-0225-3	25947	High Fe Basalt	NQ	47.3312	47.2954
25947-0225-4	25947	High Fe Basalt	NQ	47.3558	47.3254
25947-0226-1	25947	High Fe Basalt	NQ	47.3403	47.2914
25947-0301-1	25947	High Fe Basalt	NQ	47.4037	47.3830
25947-0301-2	25947	High Fe Basalt	NQ	47.2627	47.2273
25986-0304-1	25986	Basaltic Komatiite	NQ	47.3220	47.2835
25986-0304-2	25986	Basaltic Komatiite	NQ	47.3341	47.3105
25986-0304-3	25986	Basaltic Komatiite	NQ	47.3354	47.2812
25986-0305-1	25986	Basaltic Komatiite	NQ	47.3550	47.3333
25986-0305-2	25986	Basaltic Komatiite	NQ	47.3784	47.3492
25986-0305-3	25986	Basaltic Komatiite	NQ	47.3113	47.2710
25986-0311-1	25986	Basaltic Komatiite	NQ	47.3305	47.2750
25986-0311-2	25986	Basaltic Komatiite	NQ	47.3159	47.2577
25986-0311-3	25986	Basaltic Komatiite	NQ	47.3659	47.3090
25986-0311-4	25986	Basaltic Komatiite	NQ	47.3892	47.3515

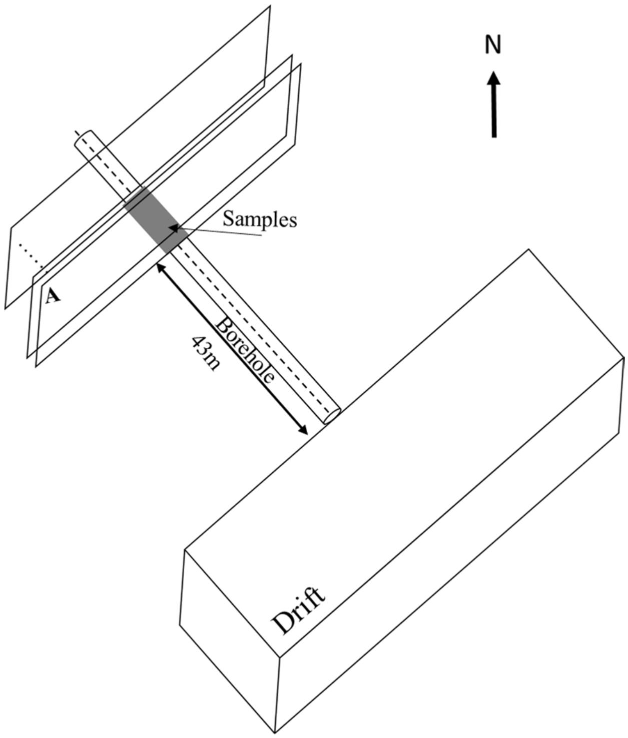

Fig. 14 Illustration of investigation stress planes (Borehole #25986)

4.2.2 Results of case study 2

Like case study 1, the test results can be applied to Eq. (1) to calculate differential principal stress. In this case, the rock type from the same borehole remains the same, and thus, the results between different samples are comparable. The NQ size rock cores belonging to the basaltic komatiite type extracted from Borehole #25986 from 43 to 51 m (10 samples) were used to conduct differential stress analysis. Figure 14 illustrates the planes for stress investigation. The elastic properties are $E = 83.3$ GPa and $\nu = 0.13$. As shown in Table 11, the results are promising. Differential stress exhibits a trend of increase with depth (Fig. 15). Differential stress variation on Fig. 15 can be caused by nearby mining activities. The location of borehole with respect to mine workings was not disclosed by the mine.

4.3 Practical application of differential stress

As the Canadian mining operations continue to reach deeper deposits, in-situ stresses become higher, the risk of violent brittle failure or rockburst of hard rock becomes high. The differential stress can be used to determine the maximum shear stress expressed as:

Table 11 Summary of differential stresses (Borehole ID: 24986)

Sample ID	$\sigma_{max} - \sigma_{min}$ (MPa)	Depth (m)
25986-0305-1	33.82	43.00
25986-0304-2	36.73	44.00
25986-0304-1	59.97	45.00
25986-0305-3	62.92	46.00
25986-0305-2	45.44	46.50
25986-0304-3	84.58	46.80
25986-0311-1	86.59	47.00
25986-0311-2	90.81	48.00
25986-0311-3	88.66	49.00
25986-0311-4	58.69	50.00

Table 12 Potential rock damage based on BSR

BSR	Rock mass damage	Potential for strain bursting
0.35	No to minor	No
0.35 to 0.45	Minor (e.g., surface spalling)	No
0.45 to 0.6	Moderate (e.g., breakout formation)	Minor
0.6 to 0.7	Moderate to major	Moderate
> 0.7	Major	Major

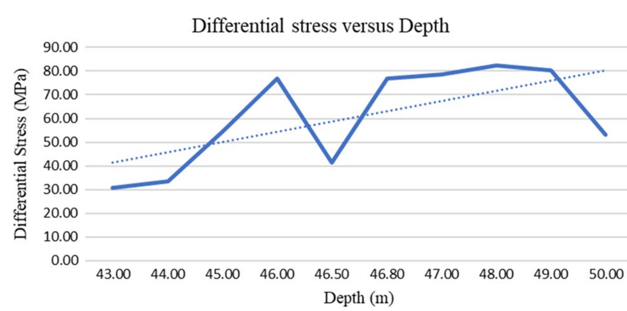

Fig. 15 Differential stress changes with depth

$$\text{Maximum shear stress} = \frac{(\sigma_1 - \sigma_3)}{2} \quad (3)$$

where σ_1 and σ_3 are the major and minor principal induced stresses.

Also, combining the differential stress with UCS of an intact rock sample (UCS_{intact}) it is possible to obtain the brittle shear ratio (BSR), which is a commonly used as a strainburst instability indicator in hard rock mines.

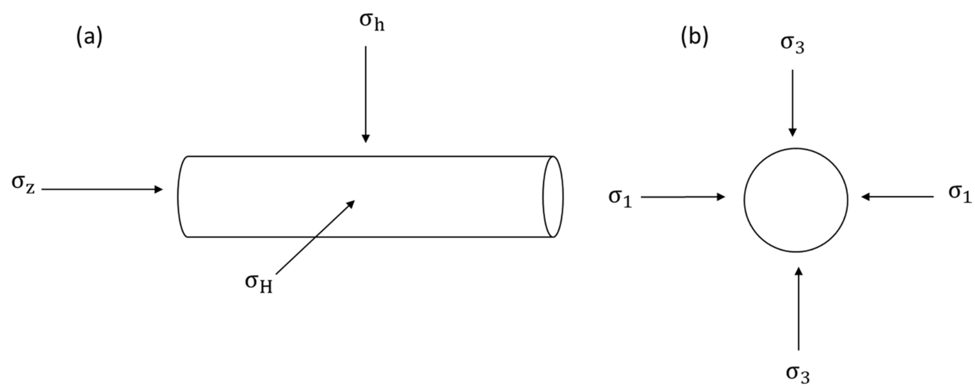

Fig. 16 Illustration of principal stresses on the rock core. **a** Rock core subject to the 3-direction in-situ stresses; **b** The cross-sectional view of rock core with principal stresses

$$\mathrm{BSR} = \frac{\left(\sigma_1 - \sigma_3\right)}{\mathrm{UCS}_{\mathrm{intact}}} \tag{4}$$

The rock damage level associated with ranges of the BSR was developed by Castro et al. (2012) (Table 12).

In Canadian mines, the vertical stress is normally smaller than the two horizontal stresses based on the Canadian shield stress database. As shown in Fig. 16, in the case of a sample retrieved far from the free face, which means σ_z is greater than σ_y, then the σ_H and σ_h illustrated in Fig. 2 will naturally become σ_1 and σ_3. Thus, it is practical to use diametral core deformation to determine the differential stress and calculate BSR for the instability analysis of brittle rock mass.

5 Discussion and conclusions

Using diametral core deformation to conduct stress analysis requires high precision of the measuring unit and the proper experimental design since every 1 µm change of the rock diameters will affect 1%–3% of the stress results. The two case studies are carried out applying the diametral core deformation analysis to estimate the differential stresses. It is shown that it is feasible to measure and use diametral rock core deformation to investigate the stresses in underground mining. The first case study reveals that the larger the rock core, the better the repeatability of the deformation measurement. That is, large cores with large diametric deformations are likely to lead to more accurate stress estimates. The second case study shows a trend of increasing differential stress with depth; the variation of differential stress may be caused by nearby mining activities. Finally, it is shown that the diametral core deformation also can be employed to determine the strainburst potential of brittle rock in terms of maximum shear stress and the brittle shear ratio.

Although diametral rock core deformation analysis provides a simple and practical method to determine the differential stresses, the following should be noted.

(1) This study considers rock has a perfect linear elastic and isotropic behavior, which is not always the case.
(2) The rock diametral deformation and fracture caused by stress release can be affected by the mineral components (Gao et al. 2021). The principal stresses cannot be determined with proposed methodology if the deformation is greatly influenced by the cracks (Funato and Ito 2017).
(3) This method can be adopted to determine the principal stresses acting on the plane that parallel to the mining face. Thus, the core orientation has to be known when conducting the analysis.

Author contributions Both authors read and approved the final manuscript.

Declarations

Competing interests The authors declare that they have no competing interests.

References

Amadei B (1984) In situ stress measurements in anisotropic rock. Int J Rock Mech Min Sci Geomech Abstracts 327–338

Brady B, Brown E (2006) Methods of stress analysis. In: Brady BHG, Brown ET (eds) Rock mechanics for underground mining, 3rd edn. Springer, Dordrecht, pp 165–196

Castro L, Bewick RB, Carter TC (2012) An overview of numerical modelling applied to deep mining. In: Innovative numerical modelling in geomechanics. Taylor & Francis Group, London, pp 393–414

Funato A, Ito T (2017) A new method of diametrical core deformation analysis for in-situ stress measurements. Int J Rock Mech Min Sci 91:112–118

Gao G, Li Z, Chang C (2021) Numerical simulation of diametrical core deformation and fracture induced by core drilling. Arab J Geosci 15–59

Kaiser PK, Diederichs MS, Martin CD, Sharp J, Steiner W (2000) Underground works in hard rock tunnelling and mining. GeoEng2000, Technomic Publ. Co., pp 841–926

Ziegler M, Valley B (2021) Evaluation of the diametrical core deformation and discing analyses for in-situ stress estimation and application to the 4.9 km deep rock core from the Basel Geothermal Borehole, Switzerland. Rock Mech Rock Eng 54:6511–6532

Publisher's Note Springer Nature remains neutral with regard to jurisdictional claims in published maps and institutional affiliations.